Journal of Alloys and Compounds 488 (2009) L1–L5

Contents lists available at ScienceDirect

Journal of Alloys and Compounds

journal homepage: www.elsevier.com/locate/jallcom

Letter

Interfacial morphologies between NiO–YSZ fuel electrode/316 stainless steel as the interconnect material and B–Ni3 brazing alloy in a solid oxide fuel cell system☆

Sungkyu Lee[a,b,*], Kyoung-Hoon Kang[a], Hyun Seon Hong[a], Yongseung Yun[a], Jae-Hwan Ahn[b]

[a] Plant Engineering Center, Institute for Advanced Engineering, 633-2 Goan-ri, Baegam-myeon, Cheoin-gu, Yongin-si, Gyeonggi-do, 449-863, Republic of Korea
[b] Division of Chemical and Materials Engineering, Ajou University, 5 Wonchon, Youngtong, Suwon, 443-749, Republic of Korea

ARTICLE INFO

Article history:
Received 5 June 2009
Received in revised form 12 August 2009
Accepted 13 August 2009
Available online 25 August 2009

Keywords:
Active brazing
Interfacial morphology
NiO–YSZ cermet
B–Ni3 brazing filler alloy
Magnetron plasma sputtering deposition

ABSTRACT

Joining of NiO–YSZ cermet with 316 stainless steel was carried out using B–Ni3 brazing alloy (4.5 wt% Si, 3.2 wt% B, 0.06 wt% C, 0.02 wt% P, Ni-balance, m.p. 982–1038 °C) to realize reliable sealing of the NiO–YSZ cermet anode/316 stainless steel interconnect structure in a SOFC. In the present research, interfacial (chemical) reactions during brazing at the NiO–YSZ/316 stainless steel interconnect were promoted by either of the two processing methods, (a) addition of an electroless nickel-plate to NiO–YSZ cermet as a coating or (b) deposition of titanium layer onto NiO–YSZ cermet by magnetron plasma sputtering method, with relevant process variables and procedures optimized during either of the pre-processing. Brazing was performed in a cold-wall vacuum furnace at 1080 °C under vacuum level of 10^{-3} Torr. Post-brazing examination of interfacial morphologies between NiO–YSZ cermet and 316 stainless steel was made using SEM and EDS. The results indicate that B–Ni3 brazing filler alloy was fused fully during brazing and continuous interfacial layer formation significantly depended on the method of pre-coating NiO–YSZ cermet. The inter-diffusion of elements was possibly promoted by titanium-deposition which reduced the diffusion reaction thickness of the interfacial area to less than 16 μm compared to 180 μm for electroless nickel-deposited NiO–YSZ cermet.

1. Introduction

Recently, fuel cells are regarded as a primary energy generation method for their high power generation efficiency and environmental friendliness to counter soaring petroleum price and worldwide concerns on greenhouse gases. The solid oxide fuel cell (SOFC) does not require a liquid electrolyte and can be operated continuously at a high temperature with reliability. Structurally, the SOFC consists of an anode, interconnect material, cathode, and a solid electrolyte. The most commonly used anode and cathode materials are NiO–YSZ (yttria–stabilized zirconia) and LSM (LaSrMn, strontium–doped lanthanum manganate), respectively [1–3].

Cr- or Fe-based alloys are widely being considered as promising interconnect materials to replace conventional La–Ga–Cr and La–Sr–Cr oxides for their better oxidation and corrosion resistance and the compatibility of thermal expansion coefficients with those of other SOFC components. This could significantly reduce SOFC operating temperature, enabling improvement in SOFC reliability. However, reliable sealing of the NiO–YSZ cermet anode/interconnect structure in a SOFC still remains a significant engineering barrier to continuous running of SOFC for more than 2000 h [3].

In general, molten metal and alloys do not wet ceramic and cermet substrates due to the highly different nature of their interatomic bonds, especially for highly stable MgO, ZrO_2, and Al_2O_3. This is due to the much higher interfacial energy than that of the unjoined surfaces. However, a chemical reaction between the metal and the ceramic substrate could lower the overall surface energy of the metal/ceramic interface, thereby increasing its stability. In many ceramic/metal joining applications, interfacial (chemical) reactions are promoted by modifying the interface areas by the addition of active elements, such as titanium, hafnium, and zirconium. These active elements ensure the formation of chemically stable ceramic/metal interface [3,4].

For proper brazing of metal/ceramic interface, special attention must be paid to three different aspects [4]:

(a) The melting range of the brazing alloy must be lower than that of the parent substrates.

☆ Work leading to this manuscript was conducted at Institute for Advanced Engineering, Korea (IAE) and all of the legal claims for the research belong to the IAE.

* Corresponding author at: Plant Engineering Center, Institute for Advanced Engineering, 633-2 Goan-ri, Baegam-myeon, Cheoin-gu, Yongin-si, Gyeonggi-do, 449-863, Republic of Korea. Tel.: +82 31 330 7318; fax: +82 31 330 7116.
E-mail address: sklee@ajou.ac.kr (S. Lee).

0925-8388/$ – see front matter © 2009 Elsevier B.V. All rights reserved.
doi:10.1016/j.jallcom.2009.08.076

(b) The solidus point of the brazing alloy must lie above the operating temperature of the brazed joint.
(c) The brazed joint must be able to withstand the SOFC operating conditions, such as temperature and other gaseous environments.

In the present research, interfacial (chemical) reactions during brazing at the NiO–YSZ/316 stainless steel interconnect were modified by either of the following pre-processing methods which prevent further oxide formation and aid in improving wettability of the NiO–YSZ cermet surface:

(a) Addition of an electroless nickel-plate to NiO–YSZ cermet as a coating.
(b) Deposition of titanium layer onto NiO–YSZ cermet by magnetron plasma sputtering method using an optimally designed jig.

The pre-processed NiO–YSZ cermet was brazed to 316 stainless steel interconnect material by using a commercially available B–Ni3 brazing alloy and the brazed joints were subsequently sectioned and further examined by scanning electron microscopy (SEM) and energy dispersive spectroscopy (EDS) to characterize and understand the interfacial reactions occurring at the NiO–YSZ/316 stainless steel interfaces.

2. Experiment

2.1. Preparation

A commercially available B–Ni3 brazing filler alloy (4.5 wt% Si, 3.2 wt% B, 0.06 wt% C, 0.02 wt% P, Ni-balance, m.p. 982–1038 °C) in its foil (100 μm) presentation was used. Both substrates and the B–Ni3 brazing alloy were ultrasonically cleaned in acetone for about 60 min. NiO–YSZ rod was prepared by wet ball milling method, pressed and sintered at 1450 °C under Ar–5% H_2 carrier gas mixture flow for 2 h as described in detail in the previously published papers [5,6]. The NiO–YSZ rod thus fabricated was further pre-processed to promote braze adhesion by either of the two methods: (a) addition of electroless nickel plating as a coat or (b) deposition of titanium layer onto NiO–YSZ cermet by magnetron plasma sputtering method using an optimally designed jig.

2.1.1. Pre-coating of NiO–YSZ rod

2.1.1.1. Electroless nickel-coating. Ultrasonically cleaned NiO–YSZ rod was electroless nickel-plated by the following unit steps which are quite similar to the conventional procedure used by other researchers [7]:

(i) Degreasing by maintaining in a stirred 20–30% NaOH solution heated to 60 °C.
(ii) Etching in a NaF solution for 10 min at ambient temperature to break down thin surface oxides.
(iii) Catalyzation by treating in 25% HCl solution containing Sn and Pd compounds for 2–10 min at ambient to maximum 40 °C.
(iv) Acceleration by immersing in 10% H_2SO_4 solution for 30–60 s at ambient temperature.
(v) Electroless nickel plating by dipping in NiB or NiP solution for 20 min at 60 °C or 90 °C, respectively.

The NiO–YSZ rod was thoroughly rinsed in running deionized water between unit steps described above (i)–(v).

2.1.1.2. Deposition of titanium layer onto NiO–YSZ cermet by magnetron plasma sputtering method. The NiO–YSZ rod was loaded in a specially designed jig as shown in Fig. 1A and the jig assembly was suitably located inside the top of a magnetron plasma sputter coating system. The chamber was evacuated to base pressure of 5×10^{-6} Torr. The sputtering target was a 10 cm diameter × 4 mm thickness titanium disk (99.9% purity) and the NiO–YSZ rod was uniformly sputter-deposited to 0.5 μm for 35 min at the rate of 2.5 Å/min. The 4 in diameter unbalanced magnetron sputter source generated titanium target power in bipolar pulsed mode and target surface magnetization of 0.7 A and 500 gauss, respectively. The distance between unbalanced magnetron source and the NiO–YSZ rod was maintained at about 70–80 mm and the magnetic field was optimally generated by computer simulation. The NiO–YSZ jig assembly was heated to and maintained at 200 °C by a combination of halogen lamp heaters and Ar plasmas. To improve titanium coating uniformity and avoid excessive heat build-up in the NiO–YSZ, the jig assembly was rotated at maximum 20 rpm.

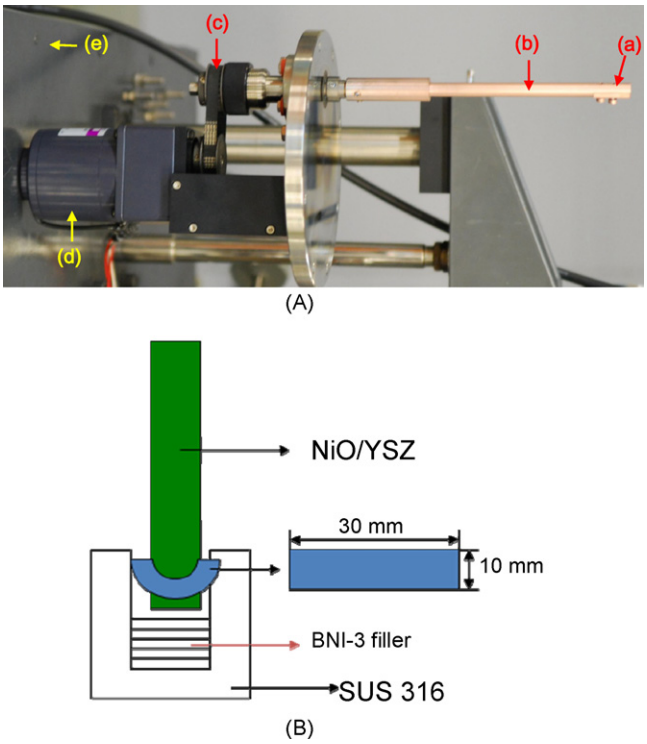

Fig. 1. (A) A specially designed jig for deposition of titanium layer onto NiO–YSZ cermet rod by magnetron plasma sputtering. It exactly shows actually set jig orientation: (a) screwed end-stopper to attach left-half portion of ∞ shaped wire assembly (not shown). A hollowed-out NiO–YSZ cylinder of (B) was slid into the right-half portion of the wire assembly; (b) rotating spindle; (c) pulley mechanism to rotate spindle at 20 rpm; (d) electric motor to drive rotating spindle; (e) left arrow points to the wall of magnetron plasma sputter coating system (sputtered titanium flux is perpendicular to the axis of the rotating spindle (b)). (B) Approximate cross-section of finally prepared NiO–YSZ/316 stainless steel interconnect assembly for brazing.

2.1.2. Final processing before brazing

The pre-coated NiO–YSZ rod was further prepared and processed for optimization of actual brazing. Fig. 1B shows approximate cross-section of finally prepared assembly of NiO–YSZ/316 stainless steel interconnect. B–Ni3 brazing filler alloy foil (100 μm thick) was cut into disk forms which were piled at the bottom of hollow 316 stainless steel fixture. 30 mm × 10 mm B–Ni3 brazing filler alloy strip was also cut out and wrapped around the lower part of the pre-coated NiO–YSZ rod.

Controlled environment affords maximum wetting and braze flow inhibitors, stop-off compound (Green, type I (Aimtek, Inc.)), were applied to mask off areas of the assembly parts, such as holes and threads, where excess flow of the filler metal would be undesirable. In the present research, stop-off compound was applied both at the tip of NiO–YSZ rod and outside area of 316 stainless steel fixture. See Fig. 1B for details of the NiO–YSZ rod/316 stainless steel interconnect assembly.

2.2. Furnace brazing and post examination

NiO–YSZ/316 stainless steel interconnect assembly was installed in a typical cold-wall vacuum furnace to perform actual brazing under vacuum of 10^{-3} Torr. The brazed assembly was cold-mounted and cut using a diamond saw, both vertically and horizontally before examination of interfacial morphologies between NiO–YSZ cermet and 316 stainless steel by scanning electron microscopy (SEM) and energy dispersive spectroscopy (EDS), both using Model LEO SUPRA 55 of Carl Zeiss, Germany. EDS analyses of the brazed joint is carried out to detect elements of Ni, Fe, and Zr down the marker line of Fig. 2b and to infer the post-brazing reaction phases in the NiO–YSZ/316 stainless steel joint, Figs. 2a and 3.

3. Results and discussion

Figs. 2b and 3 show the micro-structural characteristics of the interfaces in the brazed NiO–YSZ/B–Ni3 alloy/316 stainless steel joints. Regardless of pre-processing method, either electroless nickel plating or deposition of titanium via magnetron plasma sputtering, B–Ni3 brazing alloy was fused fully and diffusion occurred to produce a continuous interfacial layer between NiO–YSZ cer-

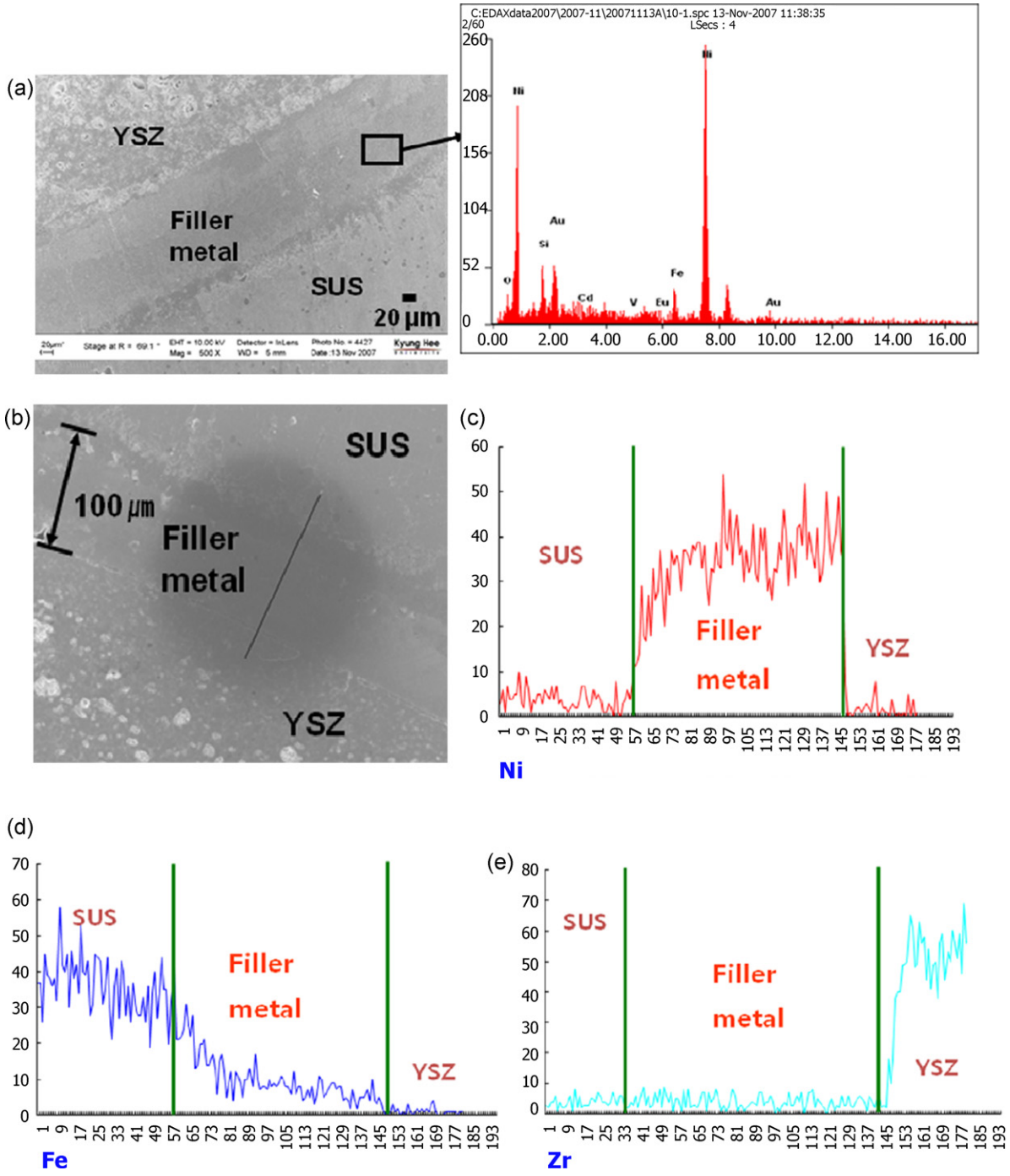

Fig. 2. Post-brazing EDS analyses of electroless nickel-plated NiO–YSZ/B–Ni3/316 stainless steel assembly: (a) micro-structural characteristics of the brazed interface and EDS elemental peaks; (b) micro-structural characteristics of the brazing filler alloy and marker line for EDS analyses of (c) Ni, (d) Fe, and (e) Zr. Ordinate and abscissa of (c)–(e) signify relative intensity of EDS elemental peak and distance across marker line in (b), respectively.

met rod and 316 stainless steel fixture. Three clearly identifiable regions have formed due to interactions between the B–Ni3 brazing filler alloy and the substrates. Although details on grain size in the interfacial layer of fused B–Ni3 filler metal region is not easily distinguishable from Figs. 2b and 3, it is strongly inferred that the interfacial layer consisted of finer grains than those of 316 stainless steel because B–Ni3 filler metal alloy completely fused during brazing and subsequently solidified perhaps rapidly during comparatively fast furnace cooling of about 21 °C/min [8–10]. EDS analysis of the joint is also carried out to investigate diffusion reaction of Ni, Fe, and Zr in the brazed joint as shown in Fig. 2c–e, which identify Ni, Fe, and Zr peak intensity variations across the brazed bonds.

3.1. *Interface reactions in electroless Ni-plated NiO–YSZ/B–Ni3/316 stainless steel*

The thickness of the interfacial layer is about 180 μm as measured by SEM/EDS, Fig. 2a. EDS analysis of Fig. 2a has revealed that the brazed joint contains more of Ni and less of Fe. It could be reasonably well assured that the EDS peak sizes for Ni and Fe within B–Ni3 alloy are directly proportional to respective compositions of

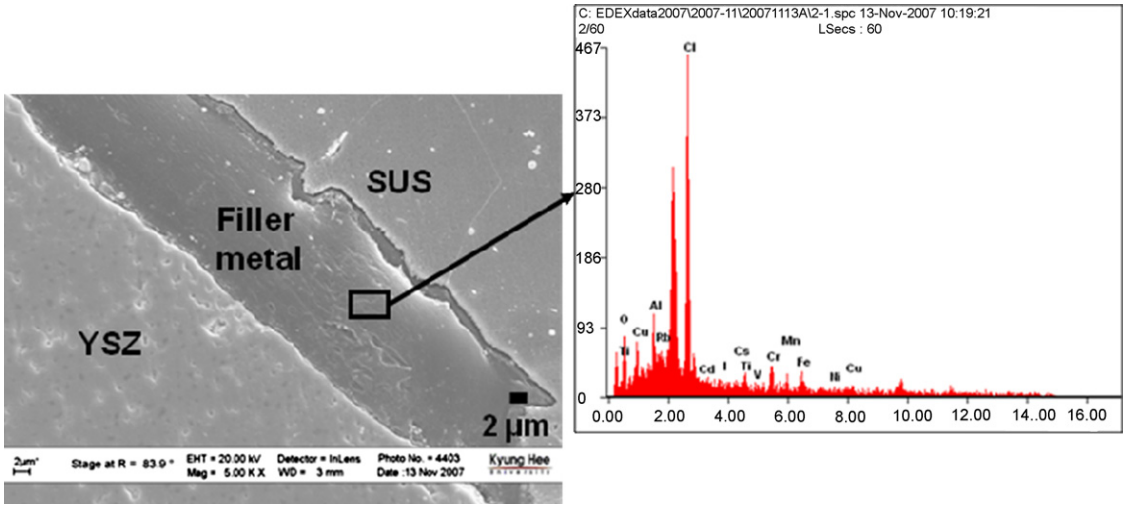

Fig. 3. Post-brazing EDS analysis of Ti-deposited NiO–YSZ/B–Ni3/316 stainless steel assembly: micro-structural characteristics of the brazed interface and EDS elemental peaks.

Ni and Fe in the B–Ni3 brazing filler alloy. Therefore, one interesting fact is observed: although inter-diffusion of Ni from B–Ni3 was not significant, Fe noticeably diffused from the 316 stainless steel to B–Ni3 brazing filler alloy section. Besides, it is highly questionable that significant amount of electroless-plated nickel diffused from NiO–YSZ cermet into 316 stainless steel up the concentration gradient as shown in Fig. 2c. This is further substantiated by missing Zr peak in Fig. 2a: very little zirconium, if any, has diffused into 316 stainless steel across the B–Ni3 brazing filler alloy and the zirconium EDS peaks of Fig. 2e in 316 stainless steel and B–Ni3 brazing filler alloy regions are too weak to signify any measurable diffusion flux of zirconium from NiO–YSZ cermet. Although nickel mapping of the electroless nickel-plated NiO–YSZ cermet was not performed, it is strongly inferred, in view of the fabrication procedure for NiO–YSZ cermet described in Section 2.1.1 and result of Ref. [7], that an amorphous and fairly continuous Ni layer was deposited on the NiO–YSZ cermet which was sintered at 1450 °C to fully dense state prior to electroless nickel-plating. Therefore, possibility of patchy and discontinuous nature of electroless-plated nickel film could thus be regarded as being unlikely.

It is well known that interfacial strength of brazed joint, B–Ni3 in the present research, is directly related to inter-diffusion of elements from brazing filler alloy to either side of it [7–10], into NiO–YSZ cermet and the 316 stainless steel, which would relieve the stress concentration in the interface. Thus, the elemental distribution of Fig. 2c–e could be regarded as a qualitative indication of interfacial bonding integrity [7] and electroless Ni-plated NiO–YSZ/B–Ni3/316 stainless steel joint would most certainly result in insufficient inter-diffusion of Fe and Zr to the B–Ni3 brazing filler alloy and many occurrences of poorly bonded brazed joint.

3.2. *Interface reactions in Ti-deposited NiO–YSZ/B–Ni3/316 stainless steel*

Fig. 3 shows that brazed joint thickness has been reduced to less than 16 μm which is quite contrary to Fig. 2a. From Fig. 3 it can be seen that the B–Ni3 brazing filler alloy reacted with the titanium deposited onto the NiO–YSZ cermet in a rather noticeable manner. From EDS analysis, it is possible to infer that the B–Ni3/NiO–YSZ cermet reaction led to the precipitation of several distinct phases out of the originally single phase materials and solid solution of titanium and nickel presumably formed at the brazed joint [8–10]. It is also important to note that EDS analyses tend to overestimate the presence of light elements such as oxygen and chlorine in Fig. 3. The titanium peak size in Fig. 3 is almost comparable to that of iron, possibly indicating the presence of solid solution in the brazed joint.

Unlike electroless nickel-plated NiO–YSZ discussed in Section 3.1, extensive diffusion of titanium into the 316 stainless steel across the brazing filler alloy interlayer is strongly inferred from Fig. 3. It is also to be noted that extensive diffusion of nickel into NiO–YSZ cermet could have occurred from the brazing filler alloy. Therefore, deposition of titanium on the NiO–YSZ significantly promoted inter-diffusion of Ni from the brazing filler alloy, which is partially justified in view of Fig. 3 and is quite contrary to Fig. 2c.

Significantly improved interfacial integrity as exemplified by continuous interfacial layer of Fig. 4 between NiO–YSZ cermet and 316 stainless steel is thus attributed to beneficial effect of titanium deposition on the NiO–YSZ cermet, which might have promoted inter-diffusion of Ni into both of the 316 stainless steel and NiO–YSZ cermet as shown by Fig. 3. In view of other researchers' analysis [11], it is also strongly inferred that the as-sputtered film of titanium is amorphous and uniform. Although reactivity of sputter-deposited titanium with the NiO–YSZ substrate was not experimentally confirmed in the present research, it is also regarded as contributing to interfacial integrity of Fig. 4 [11]. However, the effect of extensive diffusion of nickel observed in the present research on the reactivity of sputter-deposited titanium

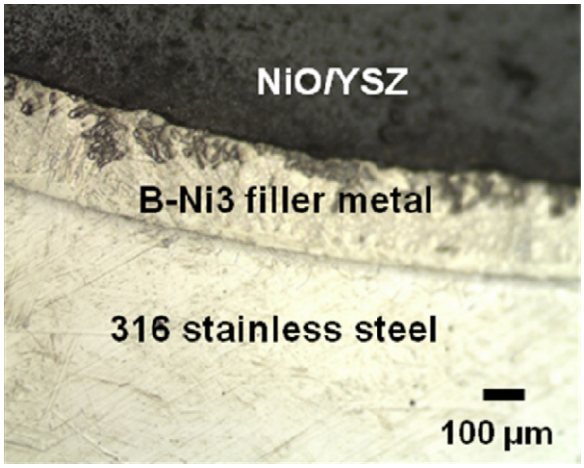

Fig. 4. Optical micrograph image of Ti-deposited NiO–YSZ/B–Ni3/316 stainless steel assembly, clearly showing integrity of brazed joint.

should be explained and other researchers' analysis [12] is referred to, where Ni (2.2 μm)/Ti (0.2 μm)/YSZ system was fabricated and interfacial reactions investigated. After annealing for 1 h at 1250 °C in an Ar–4 vol.% H_2 atmosphere, partial melt of metallic phase on the YSZ surface was observed [12], which is in agreement with the Ti–Ni phase diagram. Subsequent EDS analysis on the surfaces of the Ni/Ti/YSZ system showed titanium in substrate YSZ surface, most probably as a solid solution to the depth of about 3 μm. In view of their observation [12], it is highly probable that reactivity of titanium with NiO–YSZ substrate was not significantly affected by the nickel over-layer. Further research in this aspect remains to be desired.

Similar reasoning can also be applied to inter-diffusion of iron from Fig. 3 which clearly implies existence of Fe concentration gradient across the brazing filler alloy interlayer. Again, magnetron plasma sputtering deposition of titanium onto the NiO–YSZ cermet demonstrated quite beneficial effect of promoting inter-diffusion of Ni from the brazing filler alloy and that of Fe across the brazing filler alloy [13,14].

4. Summary

B–Ni3 brazing filler alloy was fused fully during brazing and continuous interfacial layer formation depended on the method of pre-coating NiO–YSZ cermet: magnetron plasma sputtering deposition of titanium onto the NiO–YSZ promoted inter-diffusion of Ni from the brazing filler alloy and that of Fe across the brazing filler alloy while titanium diffused into 316 stainless steel substrate. On the other hand, electroless nickel-coating on NiO–YSZ cermet did not demonstrate significantly noticeable effect in promoting sufficient inter-diffusion of Fe and Zr to the B–Ni3 brazing filler alloy. Therefore, titanium-deposited NiO–YSZ cermet rendered a quite strong bonding to the 316 stainless steel substrate by promoting inter-diffusion of titanium, nickel and iron. When the inter-diffusion of major constituent elements was promoted by titanium-deposition, the diffusion reaction thickness of the interfacial area was reduced to less than 16 μm compared to 180 μm observed for electroless nickel-deposited NiO–YSZ cermet.

Acknowledgments

The present research was supported by Ministry of Knowledge Economy, Materials & Components Agency, Republic of Korea. Mr. S.-D. Kim and G.-H. Kim of IAE assisted in magnetron plasma sputtering deposition and preparation of artworks (Figs. 2–4), respectively.

References

[1] B.C.H. Steele, A. Heinzel, Nature 414 (2001) 345.
[2] G.J.K. Acres, J. Power Sources 100 (2001) 60.
[3] Y.-W. Yen, C.-Y. Lee, D.-P. Huang, J.-W. Su, J. Alloys Compd. 466 (2008) 383.
[4] R. Arróyave, T.W. Eagar, Acta Mater. 51 (2003) 4871.
[5] S. Lee, K.-H. Kang, J.-M. Kim, H.S. Hong, Y. Yun, S.-K. Woo, Jpn. J. Appl. Phys. 47 (2008) 1838.
[6] S. Lee, K.-H. Kang, H.S. Hong, Y. Yun, S.-K. Woo, Int. J. Mater. Res. 99 (2008) 114.
[7] F. dal Grande, A. Thursfield, I.S. Metcalfe, Solid State Ionics 179 (2008) 2042.
[8] L. Peng, L. Yajiang, W. Juan, G. Jishi, Mater. Res. Bull. 38 (2003) 1493.
[9] C. Xia, Y. Li, U.A. Puchkov, S.A. Gerasimov, J. Wang, Vacuum 82 (2008) 799.
[10] W. Juan, L. Yajiang, S.A. Gerasimov, Bull. Mater. Sci. 30 (2007) 415.
[11] K. Kowalski, A. Bernasik, A. Sadowski, J. Eur. Ceram. Soc. 20 (2000) 951.
[12] A. Tsoga, A. Naoumidis, P. Nikolopoulos, Acta Mater. 44 (1996) 3679.
[13] G.W. Liu, W. Li, G.J. Qiao, H.J. Wang, J.F. Yang, T.J. Lu, J. Alloys Compd. 470 (2009) 163.
[14] G.W. Liu, G.J. Qiao, H.J. Wang, J.F. Yang, T.J. Lu, J. Eur. Ceram. Soc. 28 (2008) 2701.